Sum-Frequency Vibrational Spectroscopic Study of Polyimide Surfaces Made by Spin Coating and Ionized Cluster Beam Deposition

Jaeho Sung and Doseok Kim*
Department of Physics, Sogang University, Seoul, 121-742 Korea

C. N. Whang
Department of Physics, Yonsei University, Seoul, 120-749 Korea

Masahito Oh-e and Hiroshi Yokoyama
Yokoyama Nano-structured Liquid Crystal Project, ERATO, Japan Science & Technology Agency, 5-9-9 Tokodai, Tsukuba, Ibaraki, 300-2635 Japan

Received: December 9, 2003; In Final Form: March 25, 2004

Surface-specific sum-frequency vibrational spectroscopy was used to study the surfaces of polyimide thin films made by spin-coating and ionized cluster beam deposition (ICBD) methods. The surface vibrational spectra in the imide CO region were different between these samples, and the analysis showed the polymer main chains lie mainly along the surface for spin-coated samples, while they are relatively upright in an ICBD film surface. The atomic force microscopy measurement showed that the root-mean-square roughness of these polymer films was similar and not directly related to the surface structure in the molecular level.

Introduction

The polyimide (PI) has been used widely from microelectronics to aerospace applications due to its high thermal stability, excellent insulating integrity, and superior electrical and mechanical properties.[1−3] In many of these applications, the surface properties such as adhesion, interdiffusion, and wettability of the polymer are crucial.[4] For example, there are still active investigations to improve the adhesion of polyimide to metal surfaces.[5] Polyimide films coated on a glass substrate and subsequently rubbed are used to align the liquid-crystal molecules in liquid-crystal display devices.[6]

In many of the applications of the polyimide, the most popular way of making the film is printing and spin coating. However, because these are wet processes, it is difficult to control the film thickness and uniformity. And since it is necessary to use special solvents such as *N*-methyl-pyrrolidinone in the above processes, the films obtained may contain some impurities.[7] Vapor deposition offered an alternative process for the fabrication of PI films.[8,9] However, the results revealed that the prepared film contained a considerable amount of isoimide.[7,10] Moreover, precise control of the film properties is considered difficult since there are few parameters to adjust for the optimal growth condition of the film. On the other hand, the ionized cluster beam deposition (ICBD) is known to be a unique film formation technique that enables the flexible control of film properties such as molecular orientation and film crystallinity, while maintaining the chemical purity.[11]

Despite the practical importance, there has not been a careful study of the PI films made by conventional spin-coating and ICBD methods. Fluorescent X-ray emission spectroscopy showed little difference between the polymer films made by the spin-coating and ICBD methods,[12] and X-ray photoemission spectroscopy also showed almost identical spectral features, implying the surface chemical composition of these samples were quite similar.[13] However, one of the most important factors in determining the surface properties of the polymer would be its structure in the molecular scale, such as chain conformation and orientation of chemical moieties at the surface. To look into these aspects, we used sum-frequency generation (SFG) vibrational spectroscopy for these polymer surfaces.

Surface SFG has proven to be a powerful tool to probe the surfaces and interfaces of various systems.[14−18] This technique uses the second-order nonlinear optical effect, which is only allowed from the region where the inversion symmetry is broken. Thus, it is highly surface specific and well suited to probe the surface of the polymer.[18] In SFG vibrational spectroscopy, the frequency of the input IR beam can be made resonant to the molecular vibrational energy level, allowing the spectroscopic investigation of the surface. Furthermore, input/output beam polarization dependence of the signal provides the information about the orientation of surface molecules. Thus, SFG is an ideal tool for studies of chemical composition and the structure of polymer surfaces.

In this paper, we report our study on PI (poly[4,4′-oxydiphenylene-pyromellitimide], PMDA-ODA) films on SiO_2 substrates prepared by two different methods, ICBD and spin coating. Sum-frequency spectra were measured around CO vibrational resonances associated with the imide rings of PI. From these spectra, we inferred that orientational distribution of the imide rings (and hence of the PI main chain) were quite parallel to the surface for the spin-coated films, while the main chains were more upright to the air for the surface of the ICBD film. Despite the above structural differences, the atomic force microscopy (AFM) images obtained from these surfaces showed only minor differences in surface roughness.

Theory

The basic theory of SFG for surface studies has already been described elsewhere.[19,20] In this section, we give only the brief

* To whom correspondence may be addressed. E-mail: doseok@sogang.ac.kr.

10.1021/jp037762b CCC: $27.50 © 2004 American Chemical Society
Published on Web 06/26/2004

description for convenience of later discussion. The SFG output intensity in the reflection direction with input visible and infrared beams of intensities $I(\omega_{vis})$ and $I(\omega_{IR})$ is given by

$$I(\omega_{SF}) \propto |\chi^{(2)}_{eff}|^2 I(\omega_{vis}) I(\omega_{IR}) \quad (1)$$

with

$$\chi^{(2)}_{eff} = [\hat{e}(\omega_{SF})\bullet\overleftrightarrow{L}(\omega_{SF})][\hat{e}(\omega_{vis})\bullet\overleftrightarrow{L}(\omega_{vis})][\hat{e}(\omega_{IR})\bullet\overleftrightarrow{L}(\omega_{IR})]\chi^{(2)} \quad (2)$$

where $\hat{e}(\Omega)$ is the unit polarization vector and $\overleftrightarrow{L}(\Omega)$ is the transmission Fresnel factor at frequency Ω.[17] The nonlinear susceptibility $\chi^{(2)}$ is related to the molecular hyperpolarizability by

$$\chi^{(2)}_{ijk} = N_s \sum \langle(\hat{\imath}\cdot\hat{\xi})(\hat{\jmath}\cdot\hat{\eta})(\hat{k}\cdot\hat{\zeta})\rangle\, \alpha^{(2)}_{\xi\eta\zeta} \quad (3)$$

where N_s is the surface density of the molecules, i, j, and k are the unit vectors of the lab coordinates (x,y,z), ξ, η, and ζ refer to the coordinates attached to each molecule, and the brackets denote an average over a molecular orientational distribution. Near the resonance, the molecular hyperpolarizability can be written as

$$\vec{\alpha} = \vec{\alpha}_{NR} + \sum_q \frac{\vec{\alpha}_q}{(\omega_{IR} - \omega_q) + i\Gamma_q} \quad (4)$$

where $\vec{\alpha}_{NR}$ is the nonresonant contribution to the hyperpolarizability and $\vec{\alpha}_q$, ω_q, and Γ_q denote the strength, resonant frequency, and damping factor of the qth vibrational mode, respectively. Here, $\vec{\alpha}_q$ can be written in terms of the product of the infrared dipole derivartive and the Raman polarizability tensor of the qth vibrational mode, $\partial\mu/\partial Q_q$ and $\partial\alpha^{(1)}/\partial Q_q$, respectively

$$\alpha^{(2)}_{q,\xi\eta\zeta} = -\sum_{\xi\eta\zeta} \frac{1}{2\epsilon_0\omega} \frac{\partial\mu_{\xi\eta}}{\partial Q_q} \frac{\partial\alpha_\xi}{\partial Q_q} \quad (5)$$

where ϵ_0 is the permittivity of air and Q_q denotes the normal-mode coordinates. From above discussion, we have

$$I(\omega_{SF}) \propto \left| \chi^{(2)}_{NR} e^{i\phi} + \sum_q \frac{A_q}{(\omega_{IR} - \omega_q) + i\Gamma_q} \right|^2 \quad (6)$$

where ϕ is the phase difference between the resonant and the nonresonant SFG signal.

Experiment

The system for the preparation of the ICBD PI film is described in detail elsewhere.[13] Pyromellitic dianhydride (PMDA) and oxydianliline (ODA) powders filled in separate stainless steel crucibles were heated and ejected through nozzles (1 mm in diameter) to form clusters due to the adiabatic expansion process. To obtain a 1:1 stoichiometric ratio of PMDA and ODA, the crucible temperatures for forming PMDA and ODA clusters were held at 210 and 180 °C, respectively. Clusters were first ionized by the electron beam (ionization voltage V_e = 200 V) and accelerated by high-acceleration voltage (V_a = 800 V) applied between the crucibles and the substrate holder. We maintained the substrate temperature at 80 °C to form a polyamic acid film and then cured this film at 300 °C for 2 h in situ in a dry nitrogen atmosphere to form a polyimide film. The base pressure of the ICBD chamber was maintained in the low 10^{-6} Torr range during the film deposition. Figure 1 shows the chemical structure of PMDA-ODA.

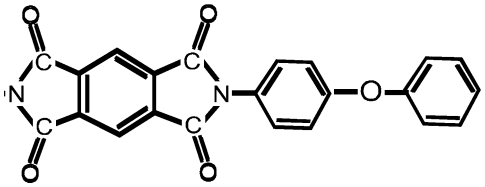

Figure 1. Chemical structure of PMDA-ODA.

The spin-coated films were made as follows. First, the PMDA-ODA polyamic acid solution was filtered with membrane filters, and then it was dropped on a substrate (Si wafer or fused quartz) to be spin coated at 3500 rpm for 60 s. The samples were then baked for 5 min at 90 °C for evaporation of solvents and 20 min at 250 °C for polyimide film formation.

For the SFG experiment, an optical parametric generator/amplifier pumped by a Nd:YAG laser was used. Briefly, a picosecond Nd:YAG laser (EKSMA, PL2143A) was used to generate a visible beam at 532 nm and a tunable IR beam around 5.7 μm, both having a 15-ps pulse width and a 20-Hz repetition rate. For the SFG experiment, two beams were overlapped at the sample surface, and the SFG output was detected in the reflection direction using the photomultiplier tube. The energies of the beams used were 60 μJ for visible and 50 μJ for tunable IR, and the beams were focused to a spot of ~1 mm diameter. The SFG signal was taken at every 2.5 cm^{-1}, and 200 laser shots were averaged at each data point. In the spectral region of this study (~1600−1900 cm^{-1}), IR beam absorption from the water vapor in the air was quite serious, and the purge box that surrounded the IR beam path was used. The dry nitrogen was put into the purge box to reduce the humidity to the 20% level before the box was sealed for the measurement. The SFG spectrum from the z-cut crystalline quartz taken at the same humidity condition was used to normalize each SFG spectrum.

Results and Discussion

The SFG spectra of PI were measured in the CO stretch region. Shown in Figure 2 are the spectra taken for the three PI films (spin coated on fused quartz, spin coated on a Si wafer, and ICBD on a Si wafer) with SSP input/output beam polarization combinations (S, S-polarized SFG; S, S-polarized visible; P, P-polarized IR). All the spectra were fitted by eq 6, and the fitted results are listed in Table 1. In the fitting for the spin-coated films, two resonance modes were used, one at 1736 cm^{-1} with a half width of 9.1 cm^{-1} and the other at 1777 cm^{-1} with a half width of 12 cm^{-1}. They can be assigned to the antisymmetric and symmetric stretch modes for coupled CO groups associated with each imide ring (shown in the inset of Figure 2), as have been already studied.[16] For ICBD films, the peaks are at 1731 cm^{-1} with a half width of 18 cm^{-1} and at 1773 cm^{-1} with a half width of 9.1 cm^{-1}. The peak shift of 4 cm^{-1} is within the spectral resolution of the setup (~5 cm^{-1} for the tunable IR beam line width) or considered to come from the difference in the environment of the surface CO groups. The difference in peak widths between ICBD and spin-coated polyimide samples may also have originated from the environmental differences. Previous studies showed that the SFG signal originated mainly from the air/PI interface,[16] and it has been proven that the quadrupole contribution to the SFG signal is negligible compared to the surface dipole contribution in polymer films.[18] Thus, the obtained spectra are considered to come only from air/PI interface. On the other hand, the infrared absorption measurement is supposed to probe the bulk polymer

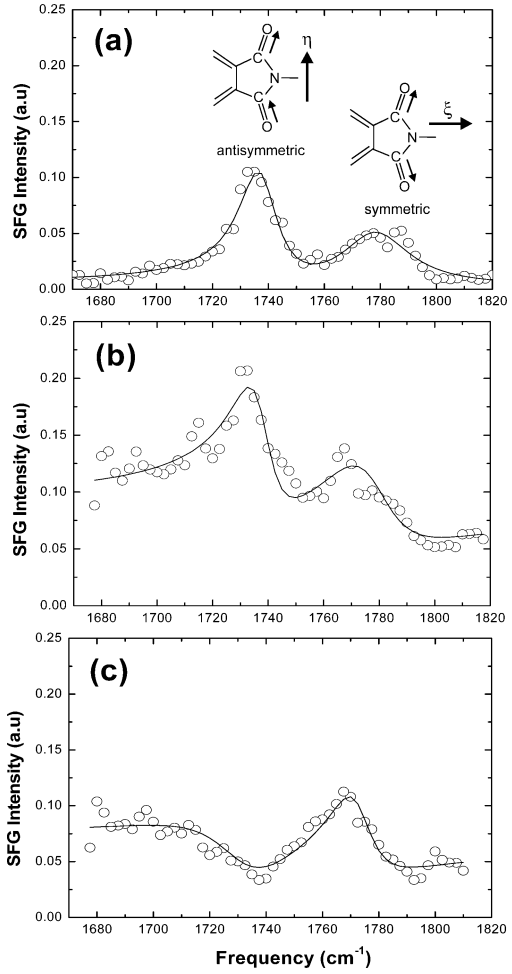

Figure 2. SFG spectra of PI films: (a) spin-coated PI on fused quartz; (b) spin-coated PI on Si wafer; (c) ICBD-PI on Si wafer. The solid lines are two-peak Lorentzian fits from eq 6. The inset shows the two corresponding imide CO normal modes in the spectra.

throughout the thickness of the film. Figure 3 shows the Fourier-transform infrared (FTIR) absorption spectra of ICBD and spin-coated PMDA-ODA samples in silicon wafer. The peaks were already assigned in previous studies as: a C−O−C asymmetric stretch for the 1242-cm^{-1} peak, a CN stretch for the 1377-cm^{-1} peak, a phenyl C−C stretch for the 1504-cm^{-1} peak, and imide CO stretches for the 1722- and 1776-cm^{-1} peaks.[21,22] In contrast to the SFG spectra, IR absorption spectra from two samples were almost the same, especially around the CO region studied with sum-frequency spectroscopy.

A notable result from the fitted values in Table 1 is that the peak strengths of A_{as} and A_s are about the same ($A_{as}/A_s = \sim 1.1-1.3$) for the spin-coated films, while the symmetric stretch peak is stronger ($A_{as}/A_s \approx 0.4$) for the ICBD film.[23] This means that the molecular orientation is different depending on the preparation methods. Figure 4a shows the angles (θ,ψ) used to define the molecular orientation with respect to the laboratory coordinates. Here, θ is the angle between the ζ axis and the surface

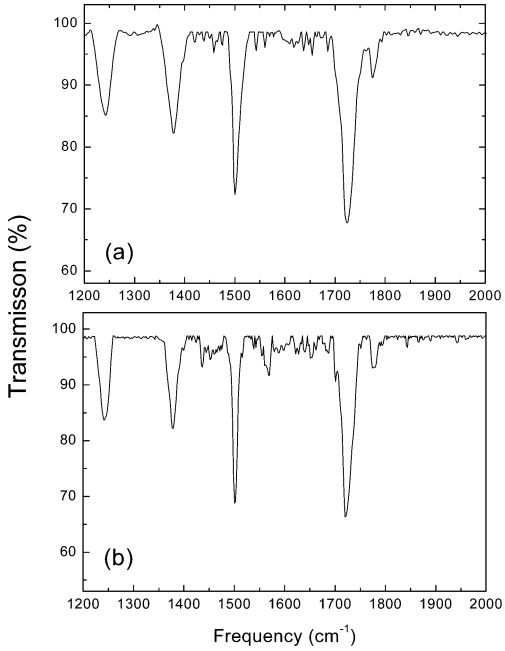

Figure 3. Infrared absorption spectra of (a) ICBD-PI on a Si wafer and (b) spin-coated PI on a Si wafer.

normal and ψ is the angle between the $\zeta-\eta$ plane and the surface normal. In the previous study with spin-coated polyimide films,[17] the ratio of antisymmetric and symmetric peak strengths from the SFG measurement was about 1.4, similar to these spin-coated samples, and the analysis was consistent with the conformation of the polymer backbone running parallel to the surface ($\theta \approx 90^\circ$ in Figure 4). However, for ICBD-PI, the symmetric stretch A_s is 2.5 times stronger compared to A_{as} so the chain conformation is expected to be different from that of the spin-coated PI surface. From the two normal modes in the spectra shown in the inset of Figure 2, the antisymmetric stretch has a dipole moment directed normal to the backbone (η direction), while the symmetric stretch has a dipole moment along the backbone (ξ) direction. Since our SFG measurement with a P-polarized infrared input beam probes the dipoles directed along the surface normal, that A_s is much stronger for ICBD-PI indicates that the backbones would be more inclined from the surface toward the normal direction. The possible molecular alignment in this case is shown in Figure 4c.

In the following, the orientation of imide rings for spin-coated and ICBD film surfaces will be deduced more quantitatively from the SFG spectra. For spin-coated films, we will formulate assuming the backbone is quite parallel to the surface and check whether it can explain our experimental result. The isolated imide core has D_{2h} symmetry, and SFG is not allowed. However, for the molecule lying nearly parallel on the surface, the upper half of the molecule is protruding out in the air, and the lower half is buried in the polymer bulk as in Figure 4b. So the "effective" symmetry of that molecular part is C_{2v}. In other terms, the two imide COs pointing in the air would mainly

TABLE 1: Fitting Parameters of the SFG Spectra

	spin-coated PI on quartz	spin-coated PI on Si	ICBD PI on Si
χ_{NR}	0.081	0.28	0.26
ϕ	3.03	2.05	0.33
A_{as}	2.0 ± 0.06 (1736 cm^{-1})	1.4 ± 0.09 (1736 cm^{-1})	2.0 ± 0.23 (1731 cm^{-1})
A_s	1.6 ± 0.10 (1777 cm^{-1})	1.3 ± 0.16 (1777 cm^{-1})	5.0 ± 0.08 (1773 cm^{-1})
Γ_{as}	9.1 cm^{-1}	9.1 cm^{-1}	18 cm^{-1}
Γ_s	12 cm^{-1}	12 cm^{-1}	9.2 cm^{-1}
A_{as}/A_s	1.26 ± 0.10	1.15 ± 0.15	0.4 ± 0.05

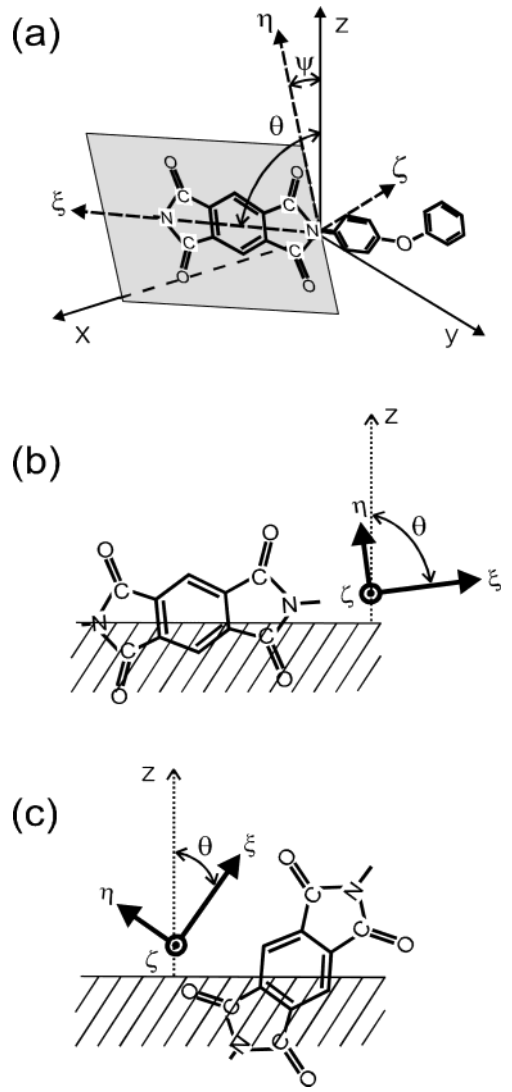

Figure 4. (a) PMDA-ODA shown with a set of molecular coordinates (ξ,η,ζ) and angles defining the relation between the laboratory coordinates (x,y,z) and the molecular coordinates (ξ,η,ζ)). (b) Configuration of the pyromellitic core nearly parallel to the surface. (c) Configuration of pyromellitic core more upright at the surface.

contribute to the SFG, and both symmetric and asymmetric imide CO stretch modes contributing to the SFG spectra have dipole moments directed along the η axis, as the two imide CO groups above in Figure 4b are considered together.[17] So for both asymmetric and symmetry stretch, the last index (corresponding to the IR field) of the sum-frequency nonlinear hyperpolarizability should be η, and the dominating molecular hyperpolarizability components are $\alpha^{(2)}_{\xi\xi\eta}$ and $\alpha^{(2)}_{\eta\eta\eta}$. Thus we have for both symmetric and antisymmetric stretch modes

$$A_{yyz,as} = -N_s(a_{as})_{\xi\xi\eta}\langle\sin^3\theta\rangle\langle\cos\psi\rangle - (a_{as})_{\eta\eta\eta}(\langle\sin\theta\rangle\langle\sin^2\psi\cos\psi\rangle + \langle\sin\theta\cos^2\theta\rangle\langle\cos^3\psi\rangle) \quad (7)$$

$$A_{yyz,s} = -N_s(a_s)_{\xi\xi\eta}\langle\sin^3\theta\rangle\langle\cos\psi\rangle - (a_s)_{\eta\eta\eta}(\langle\sin\theta\rangle\langle\sin^2\psi\cos\psi\rangle + \langle\sin\theta\cos^2\theta\rangle\langle\cos^3\psi\rangle) \quad (8)$$

To determine the tilt angle of surface molecules, we used the ratio $A_{yyz,as}/A_{yyz,s}$, which is independent of the local field factor. To obtain more exact information about the molecular orientation, spectra taken with other polarization combinations would be helpful, but the spectra with SPS polarization

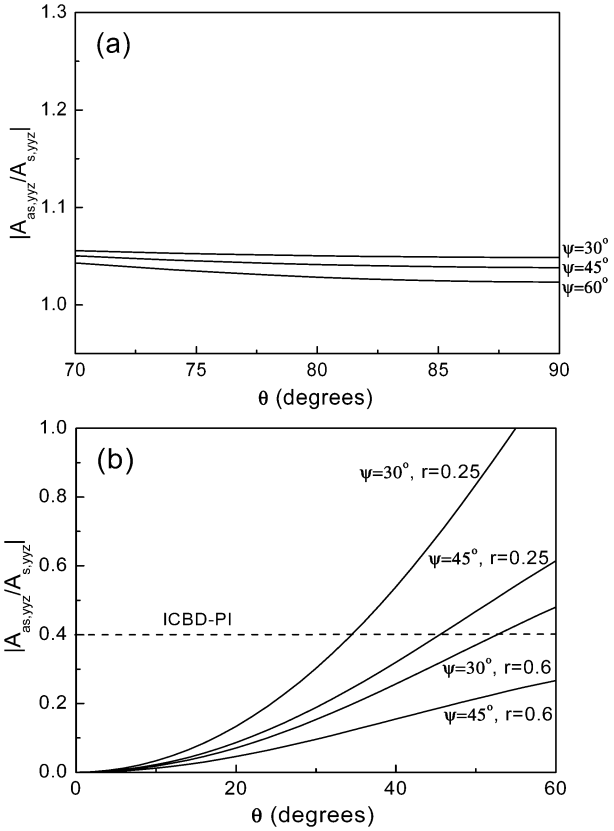

Figure 5. Calculated ratio $|A_{yyz,as}|/|A_{yyz,s}|$ of imide CO peak strengths (a) when the pyromellitic core is nearly parallel to the surface and (b) when the pyromellitic core has more angle with respect to the surface.

combinations were too small for quantitative analysis, and the determination of the peak strengths from the PPP spectra was not very accurate due to very high nonresonant background SFG signal from the samples on Si substrate. Since the ratio of hyperpolarzability values in eqs 7 and 8 are known from ref 17 as $(a_{as})_{\eta\eta\eta}/(a_{as})_{\xi\xi\eta} \approx 1.13$ and $(a_s)_{\eta\eta\eta}/(a_s)_{\xi\xi\eta} \approx 1.25$, we estimated the tilt angle of the CO groups using these values and assuming the delta-function distribution of the molecules. Shown in Figure 5a is the calculated ratio of two peak strengths with respect to θ for several fixed ψ values. Since this model is valid when the two COs in the upper half are above the bulk as in Figure 4b, θ in the graph is shown from 70 to 90°. The calculated ratio is close to our experimental value of 1.1 for tilt angles $\theta \approx 90°$ for a spin-coated sample on a Si wafer and somewhat different for a spin-coated film on quartz. The uncertainties in the previously determined depolarization ratios (ratio of hyperpolarzability values $(a)_{\eta\eta\eta}/(a)_{\xi\xi\eta}$), and the experimental uncertainties are considered to be the cause of slight disagreement. These results agree with previous results that reported polymer backbones were quite parallel to the surface for spin-coated PI surfaces,[17,21,22] while the ICBD sample, with $A_{as}/A_s \approx 0.4$, cannot have the orientation parallel to the surface.

As the calculation based on near-parallel alignment of the pyromellitic core cannot explain the ICBD-PI experimental result, we considered the possibility that the chain is not very parallel to the surface. In this case, one of the imide rings protrude out of the surface and this group solely contributes to the SFG signal, while the other imide ring across the benzene ring is buried in the bulk and is expected to contribute little to the SFG signal, as shown in Figure 4c. Since the CO groups in one imide ring only generate the SFG signal, the nonvanishing hyperpolarizability components should be changed from the previous case. As the infrared dipole is along the ξ axis for the

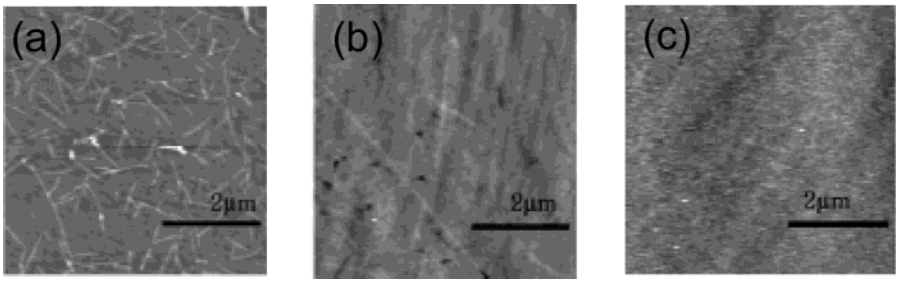

Figure 6. AFM images of (a) ICBD-PI on a Si wafer, (b) spin-coated PI on a Si wafer, and (c) spin-coated PI on fused quartz. The root-mean-square roughness values are (a) 1.3, (b) 1.5, and (c) 0.6 nm.

symmetric-stretch mode, the nonvanishing hyperpolarizability components are $a_{\xi\xi\xi}$ and $a_{\eta\eta\xi}$. For asymmetric stretch vibrations, the infrared dipole is directed along the η axis and the nonvanishing hyperpolarizability component is $a_{\xi\eta\eta}$. With this model, eq 3 immediately yields the following equations

$$A_{yyz,\mathrm{as}} = N_\mathrm{s}\{(a_\mathrm{as})_{\xi\eta\eta}\langle\sin^2\theta\cos\theta\rangle\langle\cos^2\psi\rangle\} \quad (9)$$

$$A_{yyz,\mathrm{s}} = \frac{N_\mathrm{s}}{2}\{(a_\mathrm{s})_{\xi\xi\xi}\langle\sin^2\theta\cos\theta\rangle + (a_\mathrm{s})_{\eta\eta\xi}(\langle\cos\theta\rangle\langle\sin^2\psi\rangle + \langle\cos^3\theta\rangle\langle\cos^2\psi\rangle)\} \quad (10)$$

By use of the single C=O bond with Raman depolarization ratio ranging from 0.25 to 0.6, we have $(a_\mathrm{s})_{\eta\eta\xi}/(a_\mathrm{s})_{\xi\xi\xi} = \sim 1.5-2.9$ and $(a_\mathrm{as})_{\xi\eta\eta}/(a_\mathrm{s})_{\xi\xi\xi} = \sim 0.6-2.0$ by applying the bond additive model to two CO bonds in the imide ring.[24−26] From eqs 9 and 10, the ratio of the peak strengths $A_{yyz,\mathrm{as}}/A_{yyz,\mathrm{s}}$ for the different molecular tilt angles was calculated in Figure 5b. Since this model is valid when one of the imide rings in the pyromellitic core is buried inside as in Figure 4c, θ in the graph is shown only up to 60°. With this model, the observed SFG peak strength ratio of 0.4 for the ICBD polyimide surface was compatible with the configuration of the imide ring more upright (e.g., $\theta \approx 45°$, $\psi \approx 45$ °, $r = 0.25$) at the surface than the spin-coated samples.

The previous X-ray diffraction study reported that the ICBD polyimide sample was more crystalline than the spin-coated films, with the PI film on NaCl(200) preferentially aligned along the (130) plane.[13] On the other hand, the IR absorption study showed the main chains in the spin-coated PI film is quite parallel to the substrate. Although the direct comparison is difficult with our samples being on the Si wafer compared to the previous study with NaCl substrate, the fact that the polymer chains on the surface are more upright for ICBD samples than the spin-coated samples agrees with our result.

To investigate the possible relation between the above conformation in the molecular level and the surface morphology, the surfaces of the above polymer samples were investigated using the atomic force microscope (AutoProbe CP, Park Scientific Instrument). Figure 6 shows the AFM images of the three PI films. The ICBD film has a surface roughness value of 1.3 nm. On the other hand, the root-mean-square roughness was 1.5 nm for spin-coated PI on the silicon wafer, and it was 0.6 nm for spin-coated PI on fused quartz. So the difference in surface roughness is small, and it can be concluded that the molecular conformation and backbone arrangement at these polyimide surfaces are not directly related to the surface morphology. Thin lines observed in the AFM image of the ICBD sample could be related to the crystalline domain of the film, and deserves more careful investigation.

Conclusion

In this study, we investigated the polyimide films made by spin-coating and ICBD methods using surface SFG vibrational spectroscopy. The SFG spectra in the imide CO region were different between the samples made by different methods, and the analysis showed that the polymer main chains lie mainly along the surface for spin-coated samples, while they are relatively upright in ICBD film surface. The AFM measurement showed that the rms roughness of these polymer films are not directly related to the surface structure in the molecular level.

Acknowledgment. This work was supported by the KOSEF through Quantum Photonic Science Research Center at Hanyang University. M.O. greatly acknowledges Hitachi Displays, Ltd., for financial support to purchase the laser system.

References and Notes

(1) Feit, E. D.; Wilkins, C. W. In *Polymer Materials for Electronic Applications*, ACS Symposium Series 184; American Chemical Society: Washington DC, 1982.
(2) *Polyimides Synthesis, Characterization and Applications*; Mittal, K. L., Ed.; Plenum: New York, 1984.
(3) *Recent Advances in Polyimide Science and Technology*; Weber, W. D., Gupta, M. R., Eds.; Society of Plastics Engineers, Mid-Hidson Section: Poughkeepsie, NY, 1987.
(4) Carbassi, F.; Morra, M.; Occhiellp, E. *Polymer Surfaces: from Physics to Technology*; John Wiley and Sons: Chichester, 1994.
(5) Murdey, R.; Stuckless, J. T. *J. Am. Chem. Soc*. **2003**, *125*, 3995.
(6) See, for example: Geary, J. M.; Goodby, J. W.; Kmetz, A. R.; Patel, J. S. *J. Appl. Phys*. **1987**, *62*, 4100.
(7) Lamb, R. N.; Baxter, J.; Grunze, M.; Wong, C. K.; Unertl, W. N. *Langmuir* **1988,** *4*, 249.
(8) Takahasi, Y.; Iijima, M.; Inagawa, K.; Itohi, A. *J. Vac. Sci. Technol. A* **1987**, *5*, 2253.
(9) Miyamae, T.; Tsukagoshi, K.; Matsuoka, O.; Yamamoto, S.; Nozoye, H. *Langmuir* **2001**, *17*, 8125.
(10) Salem, J. R.; Sequeda, F. O.; Duran, J.; Lee, W. Y. *J. Vac. Sci. Technol., A* **1986,** *4*, 369.
(11) Usi, H.; Yamada, I.; Takagi, T. *J. Vac. Sci. Technol., A* **1986** *4*, 52.
(12) Winarski, R. P.; Ederer, D. L.; Kurmaev, E. Z.; Shamin, S. N.; Endo, K.; Ida, T.; Moewes, A.; Chang, G. S.; Kim, S. Y.; Whang, C. N. *Thin Solid Films* **1999**, *357*, 91.
(13) Hong, C. E.; Kim, N. Y.; Kim, S. Y.; Yoon, H. S.; Kim, K. W.; Whang, C. N. *Jpn. J. Appl. Phys*. **1997**, *36*, 1715.
(14) Zhang, D.; Shen, Y. R.; Somorjai, G. A. *Chem. Phys. Lett*. **1997**, *281*, 394.
(15) Wei, X.; Zhuang, X.; Hong, S.; Goto, T.; Shen, Y. R. *Phys. Rev. Lett*. **1999**, *82*, 4256.
(16) Kim, D.; Shen, Y. R. *Appl. Phys. Lett*. **1999**, *74*, 3314.
(17) Kim, D.; Oh-e, M.; Shen, Y. R. *Macromolecules* **2001**, *34*, 9125.
(18) Wei, X.; Hong, S. C.; Lvovsky, A. I.; Held, H.; Shen, Y. R. *J. Phys. Chem. B* **2000**, *104*, 3349.
(19) Shen, Y. R. *Annu. Rev. Phys. Chem*. **1989**, *40*, 327.
(20) Shen, Y. R. *Surf. Sci*. **1994**, *299/300*, 551.
(21) Sakamoto, K.; Arafune, R.; Ito, N.; Ushida, S.; Suzuki, Y.; Morokawa, S. *J. Appl. Phys*. **1996**, *80*, 431.
(22) Hietpas, G. D.; Sands, J. M.; Allara, D. L. *Macromolecules* **1998**, *31*, 3374.

(23) Although the CO asymmetric stretch of the SFG spectrum in Figure 2a looks like a dip, such that the relative phase would be different from parts b and c of Figure 2, that peak can only be fitted by $A_{as}/A_s \approx 0.4$. As the phase of the nonresonant background of Figure 2a is different from those of parts b and c of Figure 2, the negative value of A_{as}/A_s cannot fit the spectrum satisfactorily.

(24) Hirose, C.; Yamamoto, H.; Akamatsu, N.; Domen, K. *J. Phys. Chem.* **1993**, *97*, 10064.

(25) Gisbergen, S. J. A.; Snijders, J. G.; Baerends, E. J. *J. Chem. Phys.* **1998**, *109*, 10657.

(26) Baldelli, S.; Markovic, N.; Ross, P.; Shen, Y. R.; Somorjai, G. *J. Phys. Chem. B* **1999**, *103*, 8920.